Nat Hazards (2016) 84:2071–2093
DOI 10.1007/s11069-016-2535-2

ORIGINAL PAPER

A cascading flash flood guidance system: development and application in Yunnan Province, China

Ziyue Zeng[1] · Guoqiang Tang[1] · Di Long[1] · Chao Zeng[1] · Meihong Ma[2] · Yang Hong[1,3,6] · Hui Xu[4] · Jing Xu[5]

Received: 29 December 2015 / Accepted: 12 August 2016 / Published online: 19 August 2016

Abstract Yunnan Province, located in Southwest China, suffers from massive flash flood hazards due to its complex mountainous hydrometeorology. However, traditional flash flood forecasting approaches can hardly provide an effective and comprehensive guide. Aiming to build a multilevel guidance system of flash flood warning for Yunnan, this study develops a Cascading Flash Flood Guidance (CFFG) system, progressively from the Flash Flood Potential Index (FFPI), the Flash Flood Hazard Index (FFHI) to the Flash Flood Risk Index (FFRI). First, land cover and vegetation cover data from MODIS products, the Harmonized World Soil Database soil map, and SRTM slope data are used in generating a composite FFPI map. In this process, an integrated approach of the analytic hierarchy process and the information entropy theory is used as a weighting method. Then, three standardized rainfall amounts (average daily amount in flood seasons, maximum 6 h and maximum 24 h amount) are added to derive FFHI. Further inclusion of GDP, population and flood prevention measures as vulnerability factors for the FFRI enabled prediction of the flash flood risk. The spatial patterns of the CFFG indices indicate that counties in east Yunnan are most susceptible to flash floods, which agrees with the distribution of observed

✉ Di Long
dlong@tsinghua.edu.cn

✉ Yang Hong
hongyang@tsinghua.edu.cn

[1] State Key Laboratory of Hydroscience and Engineering, Department of Hydraulic Engineering, Tsinghua University, Beijing 100084, China

[2] College of Water Sciences, Beijing Normal University, Beijing, China

[3] School of Civil Engineering and Environmental Science, University of Oklahoma, Norman, OK, USA

[4] National Meteorological Center, China Meteorological Administration, Beijing, China

[5] State Key Laboratory of Severe Weather, Chinese Academy of Meteorological Sciences, Beijing, China

[6] State Key Laboratory of Hydroscience and Engineering, Department of Hydraulic Engineering, Tsinghua University, Room 207, Beijing 100084, China

flash flood events. Compared to other approaches, the CFFG system could be a useful prototype in mapping characteristics of China's flash floods in a cascading manner (i.e., potential, hazard and risk) for users at different administrative levels (e.g., town, county, province and even nation).

Keywords Flash flood forecasting · Cascading flash flood guidance system · Flash Flood Potential Index · Flash Flood Hazard Index · Flash Flood Risk Index

1 Introduction

Flash flooding is among the most devastating natural hazards worldwide. Due to its monsoon climates and complex mountainous terrains, China faces a serious flash flooding problem, especially in the southwest. According to China Floods and Droughts Disasters Bulletin 2014 (http://www.mwr.gov.cn/zwzc/hygb/zgshzhgb), about 984 deaths per year on average were caused by flash floods (including floods in medium and small rivers) from 2000 to 2014, accounting for 73.4 % of the fatalities due to floods. Such high percentage yearly risk has underscored the need for deploying a long-due yet effective flash flood monitoring and warning system, especially in southwestern mountainous regions. A flash flood is a rapid surface water response to rainfall associated with a severe thunderstorm or a release of impounded water (e.g., dam or levee break) in a short period of time, generally within minutes up to 6 h (Hong et al. 2013). Short warning time, fast rising water levels, and high velocity make flash floods extremely dangerous to lives and property (Creutin et al. 2013). When flash flooding occurs or is deemed imminent, it is critical to issue a warning and take evacuation actions with ample time. A flash flood warning system requires knowledge of flash flooding mechanisms, geographical and socioeconomic data, accurate rainfall forecasts with enough leading time, flash flooding inventory, and efficient information dissemination.

Recent approaches to determine flash flood occurrence, including statistical models that identify statistical relationships between rainfall data and streamflow, especially neural network models, provide a basis for flash flood forecasting. These empirical models require long-term data records without the need for understanding underlying physical processes (e.g., Jiang and Shao 2010; Sahoo and Ray 2006). Therefore, results of rainfall–runoff relationships are often site-specific. Hydrological models accommodate the hydrological process to estimate streamflow over river basins and assist forecasters in making a comparison between simulated streamflow and observed flooding threshold to determine whether a warning should be issued. For example, the Sacramento Soil Moisture Accounting Model (SAC-SMA) (Bumash et al. 1973) was used at the US National Weather Service Forecast Centers as a primary operational model, and the conceptual Hydrologic MODel (HyMOD) (Boyle 2001) was used for real-time flash flood forecasting in both China and America (Chen et al. 2013). Some semi-distributed or distributed models, such as the HL-RDHM model (Koren et al. 2004) and the Coupled Routing and Excess Storage (CREST) Model (Khan et al. 2011; Wang et al. 2011a, b), were also applied to improve accuracy of flood forecasting. However, the suitability of a hydrological model depends largely on factors such as data availability, temporal and spatial resolutions of the forcing, mechanism of the model, and its computational requirements. Particularly, in situ streamflow observations for model validation are often difficult to obtain in small catchments, which impedes the development of such an approach.

Another widely used approach is the Flash Flood Guidance (FFG), which was first proposed by the River Forecast Centers (RFCs) across the USA in 1970s. It has gone through several generations, including the "Original FFG" (OFFG) (e.g., Mogil et al. 1978; Georgakakos 1987), the "Lumped FFG" (LFFG) (Sweeney 1992), the "Flash Flood Potential Index" (FFPI) (Smith 2003), the "Gridded FFG" (GFFG) (Schmidt et al. 2007) and the "Distributed FFG" (DFFG) (Clark et al. 2014). In the FFG approach, once the forecasted rainfall amount in a particular duration (e.g., 1, 3, and 6 h) over a specific basin exceeds the prescribed rainfall threshold value, a warning should be issued. The FFG rainfall threshold value is defined as the amount of rain required in a given time and area to produce bank full conditions on small streams (Sweeney and Baumgardner 1999). Given its conceptual simplicity, FFG is easy to understand, and furthermore, easy to implement since it does not require hydrological modeling. Thus, FFG alternatively provides practical means to improve flash flooding warning services (Hapuarachchi et al. 2011).

In the services of the China Meteorological Administration and the Ministry of Water Resources, determination of rainfall threshold values (or critical rainfall) has already been started at the provincial level, which can be reasonably regarded as a prototype of the FFG. However, uncertainty in their methods to determine rainfall threshold values hinders the forecasting accuracy. In China, mountainous areas account for almost two-thirds of the land area. Flash floods in these areas are often not necessarily associated with bank full conditions on small streams. As one of the FFG indices, the Flash Flood Potential Index (FFPI), mainly depending on geographical and topographical factors, is more suitable for China's topographically complex terrains where soil moisture is a less important component for flash flood occurrence (RFC Development Management Team 2003). The key to the FFPI method is to determine relative values (usually 1–10) to indicate likelihood of flash flood occurrence. Related studies on flood zoning have drawn much attention to regions prone to floods in China (e.g., Wang et al. 2011a, b, Zhang et al. 2000). Similarly, Tang and Zhu (2005) proposed a flash flood risk map for the Red River basin in Yunnan Province, which divided the study area into four categories (extremely high-, high-, medium- and low-risk zone). Lin et al. (2015) also established a flash flood hazard zoning index system for Tiaoshi Town of Chongqing City. The quality of flood maps should always be carefully validated. This could be accomplished by checking the results against historical flood events and reported flood damages (Büchele et al. 2006). However, few of these studies assessed their results with observed flood inventory data. Moreover, no comparison between results of risk assessment and the relevant losses has been comprehensively conducted to validate or demonstrate the degree of accuracy in China (Li et al. 2012). Much of the research on flash flood risk validation in other countries (e.g., Malaysia of Jiang et al. 2009; Pradhan 2010, pan-Europe of De Roo et al. 2007) has underlined the necessity of assessing the accuracy of a flood risk map with the distribution of flooded areas, refuges, residential areas, and the empirical/synthetic damage data or other flood risk maps from authoritative sources. Therefore, there is still room for improvement in flash flood risk mapping research in China.

This study first describes the development of the Flash Flood Potential Index (FFPI) by considering semi-static geo-topographical factors, taking Yunnan Province in Southwest China as a test bed. To further enhance the flash flood guidance at more comprehensive and progressive manners, two additional indices, i.e., the Flash Flood Hazard Index (FFHI) and the Flash Flood Risk Index (FFRI), are consecutively developed. Therefore, the three indices FFPI–FFHI–FFRI form the basis of the Cascading Flash Flood Guidance (CFFG)

system that progressively maps potential, hazard, and risk for flash flooding research, operation, prevention, and mitigation. The CFFG system is also quantitatively validated *using reported flash flood inventory data.* This paper is organized as follows: study area, data sets and methodology are described in Sect. 2; results are presented in Sect. 3; followed by conclusion and discussion in Sect. 4.

2 Study area, data sets, and methodology

2.1 Study area

Yunnan is one of provinces suffering from frequent and serious natural hazards in Southwest China (Long et al. 2014). Located within 97°31′–106°12′E and 20°8′–29°16′N, Yunnan is a low-latitude highland region with a total area of 383,210 km^2, 84 % of which is mountain, 10 % high plateau, and 6 % basin (Fig. 1). About 39 % of the province are mountainous areas with slope more than 25°. In the northeast and northwest of Yunnan, the dominated slope can even reach 60–80 %. The texture of most soil is loose with over 50 % of the area covered by krasnozem, which greatly contributes to the frequent occurrence of flash flooding. Jointly influenced by the East Asian summer monsoon and the Indian summer monsoon, the annual precipitation varies greatly both spatially and temporally, with 85–95 % of the rainfall occurring between May and October (Zhou and Yan 2007).

2.2 Data sets

Data sets needed in this study are:

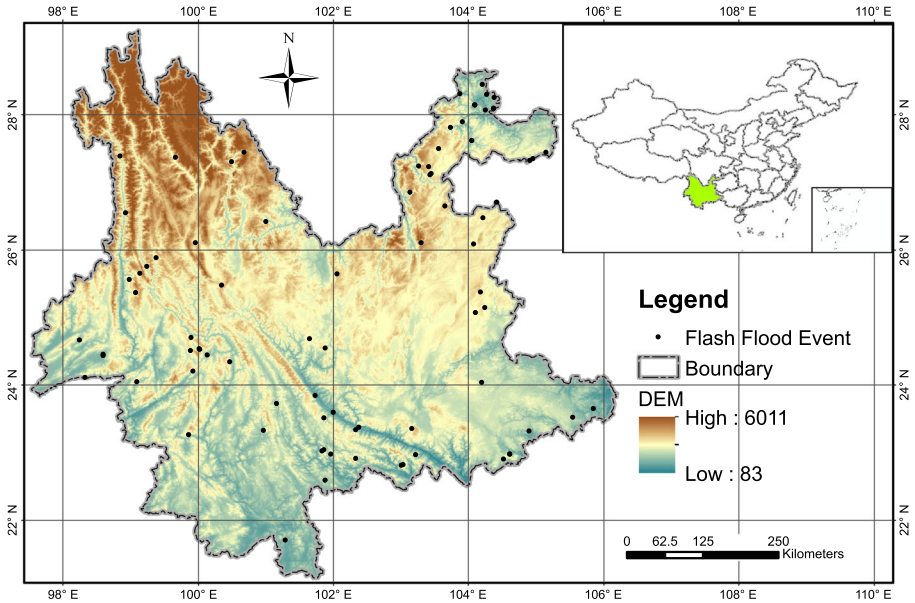

Fig. 1 DEM and observed flash flood event locations in Yunnan Province

Soil Soil characteristics were derived from soil types of Harmonized World Soil Database Version 1.2 (http://webarchive.iiasa.ac.at/Research/LUC/External-World-soil-database/HTML/index.html?sb=1). The soil map of China was provided by the Institute of Soil Science in Nanjing with 1-km spatial resolution. As infiltration rate of precipitation is greatly affected by soil texture, soil information is the percentage of sand, silt, and clay.

Vegetation cover Vegetation, particular vegetation cover, intercepts precipitation and makes the soil porous with their roots, thus influencing the infiltration process. The percent vegetation cover was derived from the Moderate Resolution Imaging Spectroradiometer (MODIS) land Vegetation Continuous Fields (VCF) Yearly L3 Global 250 m (https://lpdaac.usgs.gov/dataset_discovery/modis/modis_products_table/mod44b).

Slope Steep slopes tend to increase the flash flood damage because of the increase in runoff velocity and the decrease in runoff accumulation time. Slope data were derived from the 90-m DEM of Shuttle Radar Topography Mission (SRTM) and released by the Computer Network Information Center, Chinese Academy of Sciences (http://www.gscloud.cn/sources/?cdataid=302&pdataid=10). The SRTM DEM, produced by NASA originally, provides high quality elevation data (http://srtm.csi.cgiar.org/).

Land cover Land cover classes, particularly the urban areas with massive impervious surfaces, have significant influence on flash flood occurrence. The MODIS Land Cover Type Yearly L3 Global 500 m is a Terra + Aqua Combined land cover product, which identifies 17 classes defined by the International Geosphere-Biosphere Program (IGBP), including 11 natural vegetation classes, three human-altered classes, and three non-vegetated classes (http://modis.gsfc.nasa.gov/data/dataprod/mod12.php).

Rainfall Rainfall used in this study is the post-real-time 3B42V7 of Tropical Rainfall Measuring Mission (TRMM) era Multi-satellite Precipitation Analysis (TMPA) products, which is at a resolution of $0.25^\circ \times 0.25^\circ$ and 3 h from 2012 to 2014 (http://pmm.nasa.gov/TRMM).

Socioeconomic data Economic situation can be reflected by gross domestic product, and population in the devastated area is an important social influence on natural disasters. We collected 1-km gridded GDP and population of 2010 in Yunnan Province. The data set is provided by the Data Center for Resources and Environmental Sciences Chinese Academy of Sciences (RESDC) (http://geodoi.ac.cn/WebCn/CategoryList.aspx).

Flood prevention measure data Constructions of measures on flash flood disaster prevention for 129 counties in Yunnan were initiated in 2010 by the local authority of the Ministry of Water Resources. The prevention measures were implemented at county level, including the establishment of automatic rainfall and water level monitoring site networks basically covering all villages, the installation of simple rainfall and water level stations with alarms, and the construction of a warning system platform consisting of wireless radio, simple warning devices such as loudspeakers and whistles. The local authority also set up a fund to strengthen knowledge dissemination, training and exercise activities to prompt the residents' awareness of flash flood disaster prevention and avoidance (Sun et al. 2012).

Flash flood inventory data The observed flash flood event data are comprised of 83 flash flood events with fatalities occurring between 2012 and 2014 in Yunnan. Every event record contains the location (county or village name), timing, number of death and

missing, site description, and preliminary loss. All the information was stored in ESRI shapefile format.

The spatial resolution of these data ranges from 90 m to 1 km, and the data were resampled to a 1-km resolution in raster format.

2.3 Methodology

Figure 2 illustrates the overall methodology in developing the CFFG system. There are four steps involved in developing each of the cascading index (FFPI, FFHI, FFRI): (1) *data collection and processing;* (2) *development of single-data-type-based index value*; (3) *assignment of weights for each data type; and* (4) *calculation for the composite flash flood guidance index*. Among the four steps, the determination of composite weights for each data type is crucial. Many studies incorporated ideas of ranking and weighting to adopt semi-quantitative methods, which are simple but often useful in regional cases (e.g., Tan et al. 2007; Sinha et al. 2008; Papaioannou et al. 2015; Lee et al. 2013). In this study, an integrated weight-optimizing method is proposed based on combinations of the analytical hierarchy process (AHP) and the information entropy theory, followed by rigorously ranking probability evaluation. The methodology is described below in progressive manners from FFPI to FFHI and FFRI.

2.3.1 Development of FFPI

Based on literature review, four key input geo-topographical data types, soil, slope, vegetation cover, and land cover, were collected and processed first. Weight for each single-data-type-based FFPI (single FFPI) was determined to calculate the composite FFPI, written as:

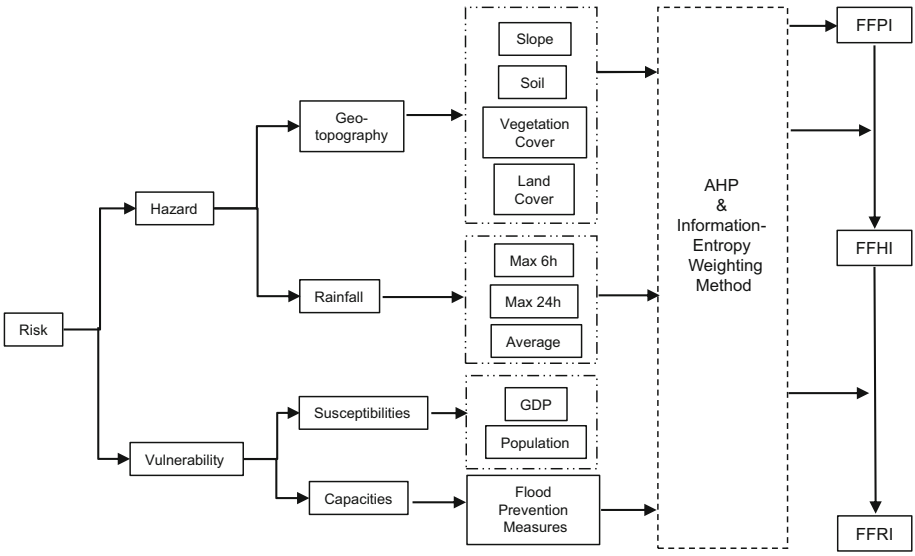

Fig. 2 Development procedures of the CFFG

$$\mathrm{FFPI} = \sum w_i \mathrm{FFPI}_i \tag{1}$$

where w_i and FFPI_i are the weight and single FFPI value for each data type, respectively, and all the w_i sum up to 1.

In the early development of FFPI, all layers were weighted equally except the slope, which was given a larger w (Clark et al. 2014). With observed flash flood event information, weights for different data types can be defined (Smith 2003). Several weighting methods have been tested, including qualitative methods like the Delphi method (Linstone and Turoff 1975), Outranking approaches (Brans et al. 1986) and the analytical hierarchy process (AHP) (Saaty 1990). Among these methods, AHP is a multiple criteria decision-making tool that has been used in most applications related with decision-making (Vaidya and Kumar 2006). Information entropy theory (Karmeshu 2003) is a measurement of the disorder degree of a system. The larger the difference of evaluating objects for an indicator, the smaller the entropy, which illustrates that this indicator provides more useful information and should be given a larger weight. It is an objective way to determine the weights (Zou et al. 2006).

The procedure of the integrated weight-optimizing method can be described as follows:

1. Calculate the weight matrix U determined by the AHP:

Basic steps involved in the AHP are discussed in a variety of research (e.g., Zahedi 1986; Saaty 1987). Assessment indicators for FFPI (equal to data types mentioned before) and the hierarchy of criteria as well as judgment matrixes for pair-wise comparisons are listed in Table 1. The weight matrix U can be expressed as:

$$U = (u_1, u_2, \ldots, u_i, \ldots, u_m) \tag{2}$$

where u_i is the weight for its corresponding data type as in Eq. 1. Where m is the number of data types, and all the u_i sum up to 1.

2. Calculate the weight matrix V determined by the information entropy theory method:

The entropy method is conducted in the following steps:

Step. 1 Calculate the information entropy for each indicator

Usually, $i = 1, 2, \ldots, n$ stands for the assessment object set, which is the grids in this study, and $j = 1, 2, \ldots, m$ for the assessment indicator set, which is the data types selected to calculate FFPI. $R = (r_{ij})_{n\times m}$ is the matrix of the original indicator values. For the jth indicator, information entropy can be defined as:

$$e_j = -k \sum_{i=1}^{n} p_{ij} \ln p_{ij} \tag{3}$$

where

$$p_{ij} = r_{ij} / \sum_{i=1}^{n} r_{ij} \tag{4}$$

when $p_{ij} = 1/n$, e_j reaches its maximum value, which is:

$$e_{\max} = \ln n \tag{5}$$

and $k = 1/\ln n$.

Table 1 Hierarchy and judgment matrix in the AHP

Goal	Criteria	Sub-criteria	Data type	Hazard							Vulnerability		
				Geo-topography				Rainfall			Susceptibilities		Capacities
				Vegetation cover	Slope	Soil	Land cover	Max 6 h	Max 24 h	Average	GDP	Population	Flood prevention measures
Flash Flood Risk Index	Hazard	Geography	Vegetation cover	1	0.2	0.5	0.33						
			Slope	5	1	3	2						
			Soil	2	0.33	1	0.5						
			Land cover	3	0.5	2	1						
		Rainfall	Max 6 h					1	2	5			
			Max 24 h					0.5	1	3			
			Average					0.2	0.333	1			
	Vulnerability	Susceptibilities	GDP								1	0.5	0.333
			Population								2	1	0.667
		Capacities	Flood prevention measures								3	1.5	1

Step. 2 Calculate the weight for each indictor:

For the *j*th indicator, weight is calculated as:

$$v_j = (1 - e_j) / \sum_{j=1}^{m} (1 - e_j) \tag{6}$$

The weight matrix V can be expressed as:

$$V = (v_1, v_2, \ldots, v_i, \ldots, v_m) \tag{7}$$

3. Calculate the final weight matrix W:

The final weight for each indicator is calculated using the formula:

$$w_i = \alpha u_i + (1 - \alpha) v_i \tag{8}$$

where α is usually determined by sensitivity analysis (e.g., Store and Kangas 2001).

The final weight matrix W can be expressed as:

$$W = (w_1, w_2, \ldots, w_i, \ldots, w_m) \tag{9}$$

To develop single FFPI values, first, each grid was given a value (from 1 to 10) for each data type. The value of 10 means the highest potential for a flash flood to occur and 1 means the lowest. We defined that *i* is 1 for soil, 2 for slope, 3 for vegetation cover, and 4 for land cover. For soil, as the infiltration rates are relatively lower in clay-dominated soils (Smith 2010), the higher percent of clay corresponds to a higher $FFPI_1$ value. For slope grids greater than 30 degrees, a $FFPI_2$ value of 10 was assigned. Equal interval was used to allocate $FFPI_2$ values of 1–9 to grids of which the slope is less than 30 degrees. For vegetation cover, the percentages were divided into 10 classes with equal intervals and each class was assigned a $FFPI_3$ value from 1 to 10. For example, $FFPI_3$ values of 1 were assigned to the 90–100 % vegetation cover class, 2 to the 80–90 % class. For land cover, it can be discretized into several general categories: (a) forested land; (b) shrub land; (c) grass land; (d) pasture and/or cropland, and (e) developed land and/or road corridors (Hong et al. 2007). Since both flash flooding and landslide are always triggered by rainfall and can often form a disaster chain, these land use/cover categories can also describe the susceptibility to flash floods, in a continuum of increasing manner. As such, $FFPI_4$ values from 1 to 10 were assigned to each category, respectively (Table 2).

2.3.2 Development of FFHI and FFRI

Flash flood risk indeed results from the dynamics of hazard and vulnerability as shown in Fig. 2. Therefore, we use FFHI and FFRI to indicate the possibility of flash flooding from perspectives of hazard and risk, respectively. This paper adopted the definition of risk from the United States glossary of basic terms related to disaster management:

$$\text{Risk} = \text{hazard} \times \text{vulnerability} \tag{10}$$

As shown in Eq. 10, *risk is a product of hazard and vulnerability.* A hazard is defined as: "A threatening event, or the probability of occurrence of a potentially damaging phenomenon within a given time period and area" (United Nations, Department of Humanitarian Affairs 1992). Several different concepts and definitions of vulnerability exist.

Table 2 Assignment of single FFPI values for different land cover types

Category	Assignment of FFPI value	Original MODIS classes	Contents
1	1	0, 15	Water bodies; permanent snow and ice
2	2	1, 2, 11	Evergreen needleleaf forest; evergreen broadleaf forest; permanent wetlands
3	3	3, 4	Deciduous needleleaf forest, deciduous broadleaf forest
4	4	5	Mixed forest
5	5	6, 7	Open and closed shrublands
6	6	8, 9	Woody savannas; savannas
7	7	10	Grasslands
8	8	12	Cropland
9	9	14	Cropland/natural vegetation mosaic
10	10	13	Urban and built-up

Overviews of the various concepts and understandings are provided, e.g. by Adger (2006), Brooks (2003) or Fuchs (2009). Generally, vulnerability is considered as social vulnerability and more likely to be measured in terms of predictive variables representing factors such as economic well-being, health and education status, preparedness and coping abilities or capacities with respect to particular hazards and so on (Brooks 2003). Coping capacities of a human system represent the potential of the system to reduce its social vulnerability and thus to minimize the risk associated with a given hazard, which refer to the means by which people use resources before, during or after the disaster to cope with its adverse consequences (Villagran de Leon 2006). Here, we adopted the concept proposed by Scheuer et al. (2011) from an end point view to integrate the adaptive/coping capacity into vulnerability and divided its influencing factors into two categories: susceptibilities and capacities.

According to the above definitions, for the element of hazard, rainfall was taken as the fifth factor to derive FFHI value based on the previous work of FFPI. We calculated the annual maximum 6- and 24-h rainfall, the average daily rainfall of the flash flood season (May to September) for each year of 2012–2014, and then averaged the 3 year's amounts. To standardize these data, each type of rainfall amount was reclassified into 1–10 by equal interval among grids and stored in three different layers as rainfall amount components. For the element of vulnerability, we considered economic and social factors as main influential factors of susceptibilities and chose the population and GDP distribution to represent the socioeconomic effect and standardized them in the same way as rainfall factors. In addition, we used prevention measures to represent coping capacities. Based on the data of flood prevention measures before May of 2013, the implementation of prevention measures of the average level for 2012–2014 can be quantified. Values were standardized into 1–10, in which 10 means the poorest in prevention from flash floods and 1 the most capable. For each county's grids, their values are unique. Information used in determining these numerical values was the density of automatic rainfall and water level monitoring site per km^2, density of simple rainfall and water level stations, number of warning devices per km^2, financial appropriation for dissemination, numbers of people

involving in training/exercise activities, and the starting time for construction of these prevention measures.

3 Results

3.1 Evaluation criterion

To evaluate performance of the three indices of the CFFG system, we introduced a skill indicator, i.e., the Rank, to present the ranking of the weighted average for indices values *in or around* flash flood locations. Locations used in this paper are accurate at the county or village level, but not precise in longitude and latitude. With no access to boundaries of villages, given that average area of villages/towns in Yunnan Province is $\sim$280 km^2, we determined *the maximum value in an area of 121 km^2 around each location (equal to 11 $\times$ 11 grids, of which the central grid is exactly the reported flash flood location) to be the composite FFPI value of its corresponding flash flood event*. Therefore, the Rank of FFPI can be calculated as:

$$\text{Rank} = \frac{\overline{\text{FFPI}} - \text{FFPI}_{\min}}{\text{FFPI}_{\max} - \text{FFPI}_{\min}} \tag{11}$$

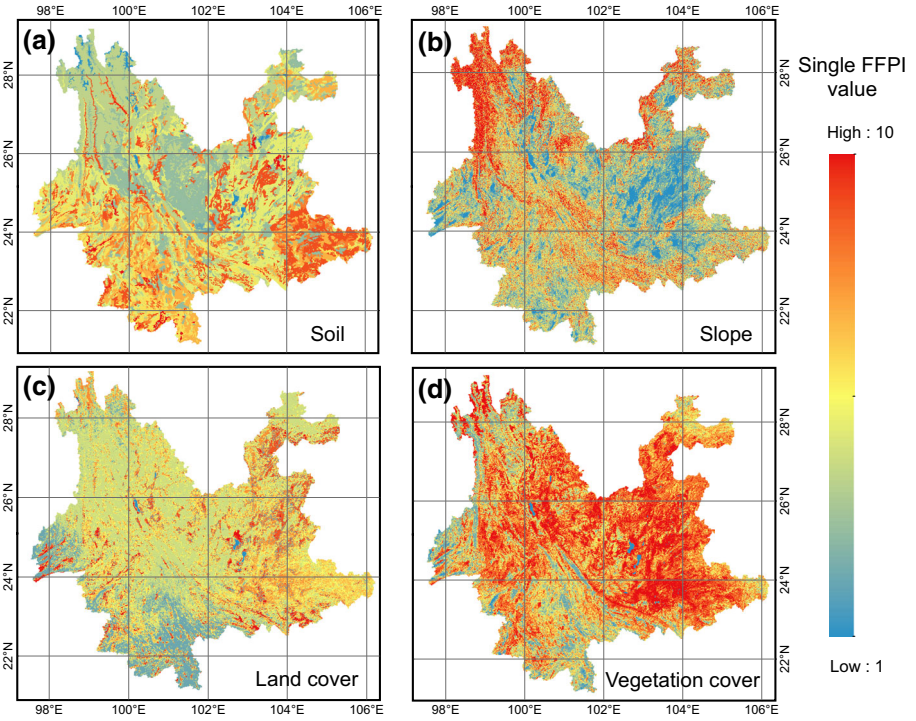

Fig. 3 Single FFPI value distribution of Yunnan Province in aspects of **a** soil, **b** slope, **c** land cover, and **d** vegetation cover

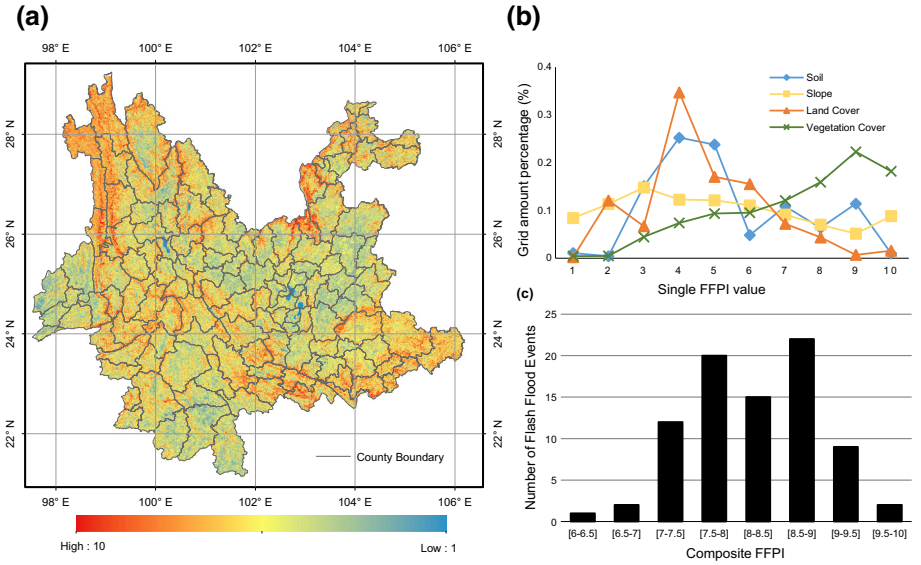

Fig. 4 Results and statistics of the composite FFPI value distribution of Yunnan Province: **a** composite FFPI value distribution, **b** gird amount percentage of single FFPI for each data type, and **c** composite FFPI value and its corresponding number of flash flood events in/around flash flood event locations

$$\overline{\mathrm{FFPI}} = \frac{1}{N}\sum_{i=1}^{M} d_i \mathrm{FFPI}_i \tag{12}$$

in which $\mathrm{FFPI}_{\max}$ and $\mathrm{FFPI}_{\min}$ is the maximum and minimum value of the FFPI in the study area and $\overline{\mathrm{FFPI}}$ is the weighted average FFPI value of all the flash flood events. Where N is the total amount of death and missing, M the total number of flash flood events, d_i the number of death and missing for the ith event, and FFPI_i the FFPI value *in or around* the

Table 3 Weights for each data type in the AHP

Indicator	Hazard 0.8[a]		Vulnerability 0.2[a]
	Geo-topography 0.75[a]	Rainfall 0.25[a]	
Vegetation cover	0.088		
Slope	0.483		
Soil	0.157		
Land cover	0.272		
Max 6 h		0.582	
Max 24 h		0.309	
Average		0.109	
GDP			0.167
Population			0.333
Flood prevention measures			0.500

[a] Weights for sub-criteria and criteria when calculating FFHI and FFRI

Table 4 Weights for different factors under the listed methods of FFPI, FFHI and FFRI, values of rank in/around flash flood event locations

Method	Hazard							Vulnerability			Rank
	Geo-topography				Rainfall			Susceptibilities		Capacities	
	Vegetation cover	Slope	Soil	Land cover	Max 6 h	Max 24 h	Average	GDP	Population	Flood prevention measures	
Entropy weighting	0.141	0.446	0.210	0.204							0.825
	0.070	0.221	0.104	0.101	0.141	0.137	0.227				0.748
	0.047	0.150	0.071	0.069	0.096	0.093	0.155	0.148	0.158	0.012	0.750
AHP	0.088	0.483	0.157	0.272							0.817
	0.066	0.362	0.118	0.204	0.145	0.077	0.027				0.632
	0.053	0.290	0.094	0.163	0.116	0.062	0.022	0.033	0.067	0.100	0.693
AHP and entropy	0.114	0.464	0.184	0.238							0.821
	0.067	0.306	0.112	0.163	0.144	0.101	0.107				0.708
	0.050	0.220	0.083	0.116	0.106	0.078	0.088	0.091	0.112	0.056	0.718

location where the *i*th event occurred. To calculate the Rank of FFHI and FFRI, methods are the same.

The final FFRI result was also analyzed at county level to further classify the 129 counties into different risk categories. The skill indictor is the percentage k_j, which can be calculated as:

$$k_j = \frac{1}{\sum_{i=1}^{T_j} \mathrm{FFRI}_i} \sum_{i=1}^{t_j} \mathrm{FFRI}_i \tag{13}$$

where $j = 1, 2, \ldots, 129$, T_j is the total number of grids of the jth county, and t_j is the number of grids with FFRI value greater than the 95 quartile of the total FFRI values of Yunnan.

3.2 Results of FFPI

The single FFPI values are shown in Fig. 3. In the southeast Yunnan, the clay-dominated soil accounts for large areas, leading to the highest potential for flash floods. Due to the mountainous terrain in the north of Yunnan and along the Yuan River, single FFPI for slope denotes that these areas are more susceptible to flash floods. Single FFPI for land cover also distinguishes urban areas from other parts. And for vegetation cover, single FFPI elucidates that a large area of Yunnan is very sparse covered with trees. Similar to

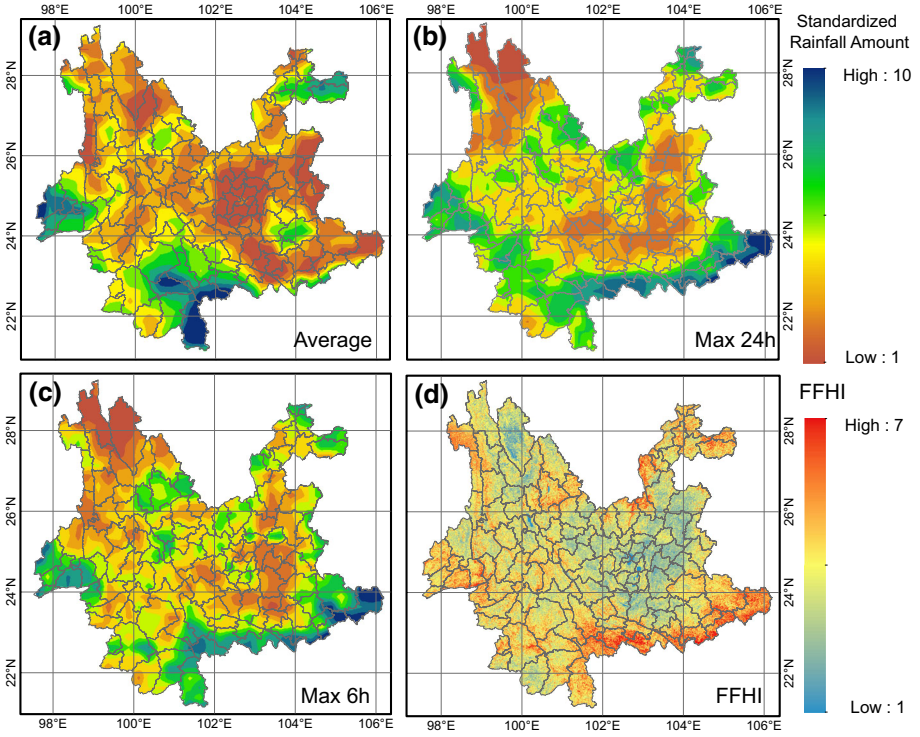

Fig. 5 Standardized rainfall amounts of **a** average daily amount in flood seasons, **b** maximum 24 h amount, **c** maximum 6 h amount of 2012–2014, and **d** spatial distribution of FFHI

single FFPI values, the composite FFPI values only represent the ranking of relative flash flood potential among grids, not quantitative relationships (Fig. 4a). More than 40 % of the total area demonstrates a FFPI above 6, with the northeast and northwest of Yunnan more susceptible to rainfall. Figure 4b shows the gird amount percentage of each single FFPI. Large areas of Yunnan have relatively low and moderate single FFPI for land cover, while high single FFPI is more common for vegetation cover. Standard deviations for the

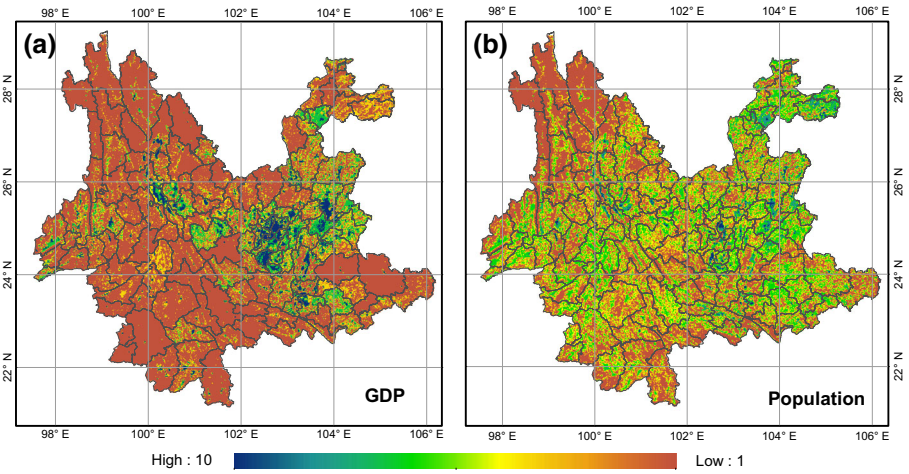

Fig. 6 **a** Standardized GDP distribution. **b** The standardized population distribution in Yunnan Province

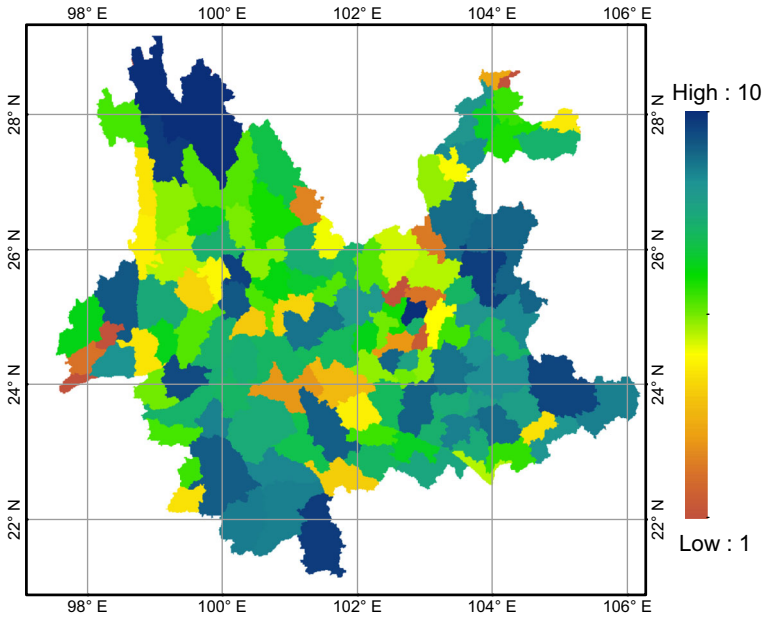

Fig. 7 Numerical value of flood prevention measures of Yunnan Province

distribution of vegetation cover, slope, soil, and land cover are 2.15, 2.68, 2.01, and 1.72, respectively. This can be a reference for the weight setting of each single FFPI.

Weights for all data types are listed in Table 3. Based on sensitivity analysis, values of α (Eq. 8) were determined to be 0.5, 0.6, and 0.5 for FFPI, FFHI, and FFRI, respectively. Table 4 shows the final weights. Slope outweighs the other three data types for FFPI development, while vegetation has the lowest weight. Rank for FFPI is *82.1 %*, showing that FFPI values and flash flood event locations have yielded a clear relationship and areas susceptible to flash floods can be easily separated from other places using the composite FFPI distribution map. Obviously from Fig. 4c, some grids show extremely high FFPI values especially in or around the historical flash flood event locations. No reported events fell in grid cells with FFPI less than 6, and about 82 % of flash flood events have FFPI values greater than 7.5, with the largest one being 9.82. However, only 2 events fell in the range of 9.5–10 and the number of events did not increase from 8.5–9 to 9–9.5. This inconsistency might be caused by the inadequate rainfall amount in these regions, or it can be explained by the fact that flash flooding would cause no damage and were not reported

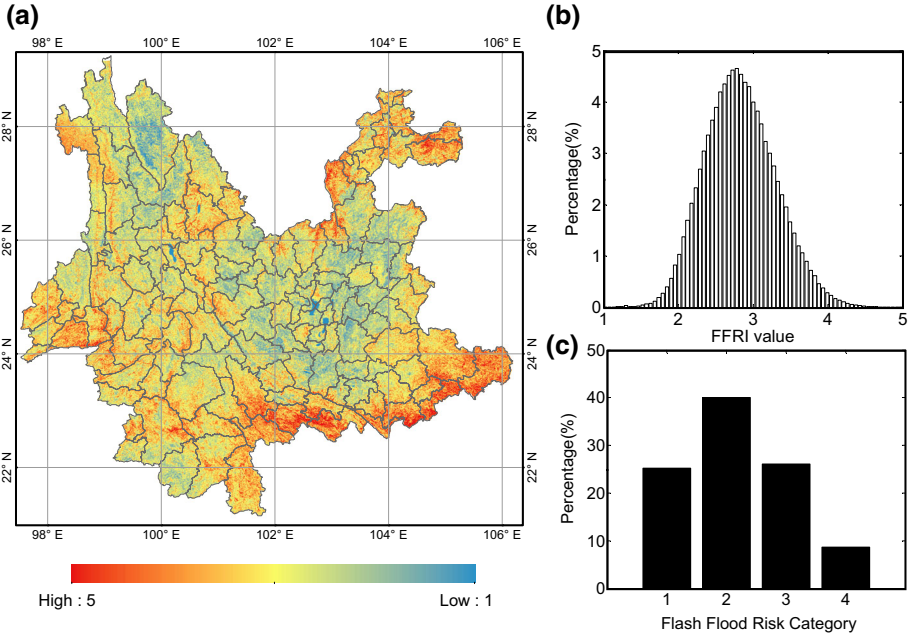

Fig. 8 a FFRI distribution of Yunnan Province. **b** Histogram of FFRI values. **c** Histogram of FFRI values classified into 4 categories

Table 5 Distribution of flash flood risk map

Category	1	2	3	4
FFRI	1–2.5	2.5–3	3–3.5	3.5–5
Percentage (%)	25.20	39.99	26.10	8.71

Table 6 Information on the top 32 counties with the highest risk of flash floods

County	Area (km^2)	k_j (%)	Vegetation cover	Slope	Soil	Land cover	Max 6 h	Max 24 h	Average	GDP	Population	Flood prevention measures
Malipo	2881	46.58					+	+				+
Luchun	3913	38.51						+	+			+
Maguan	3340	35.42	+		+			+				
Jinping	4369	31.15					+	+				+
Funing	6617	30.06					+	+				+
Hekou	1571	28.26					+	+				+
Weixin	1840	20.54	+						+			+
Zhenxiong	4792	19.05	+						+			+
Qiaojia	4160	19.01	+	+								+
Yuanyang	2843	17.13	+					+				+
Jiangcheng	4261	16.59					+	+	+			
Luxi	3642	15.46					+	+				+
Xichou	1920	14.90	+				+	+				
Dongchuan	2466	14.19	+	+	+							
Wanding	107	14.02					+	+	+			
Longling	3564	13.44					+	+				+
Guangnan	9945	13.02	+		+							+
Shuifu	541	12.20		+			+	+				
Daguan	2267	11.78	+	+								+
Mojiang	6681	11.38	+	+								+
Pingbian	2368	10.35	+	+								+
Ludian	1967	9.86	+			+						+
Zhenkang	3187	9.44	+					+				+
Ximeng	1632	9.07	+		+							+
Yiliang	3628	9.01	+						+			+
Yanjin	2627	8.87	+					+				+

Table 6 continued

County	Area (km^2)	k_j (%)	Vegetation cover	Slope	Soil	Land cover	Max 6 h	Max 24 h	Average	GDP	Population	Flood prevention measures
Shidian	2519	7.94	+		+							+
Mengna	8354	7.65					+		+			+
Simao	4896	7.64	+						+			+
Suijiang	1021	7.05		+			+	+				
Zhaoyang	2822	6.56	+			+						+
Yongsheng	6484	6.26	+				+					+

"+" indicates the dominant data type

because they occurred in an unpopulated area or a region where human systems are well adapted to cope with it (Brooks 2003).

3.3 Results of FFHI and FFRI

The value of Rank based on final weights of FFHI is *70.8 %*. After standardization, the distribution of rainfall amount (Fig. 5) changes greatly at provincial scale. The spatial pattern differs from that of the composite FFPI, especially for the average rainfall (Fig. 5a), which illustrates that the south and west of Yunnan have a higher possibility of large precipitation for flash flooding to occur. Thus, the value of Rank decreased. However, it also reveals a significant agreement between the FFHI distribution and its spatial pattern of flash floods (Fig. 5d). The values of GDP and population are show in Fig. 6. With concentrated population and high GDP, the east-central Yunnan has higher value, while the value of flood prevention measures there is relatively lower than other parts (Fig. 7). The final FFRI value of Yunnan ranges from 1 to 5 (Fig. 8a). FFRI demonstrates the spatial pattern of flash flood risk and the hot spots of high-risk regions, mainly located in the northeast and southeast of Yunnan. The result of the Rank of FFRI reaches *71.8 %*. This continuous scale of numerical indices of FFRI can be further classified into several

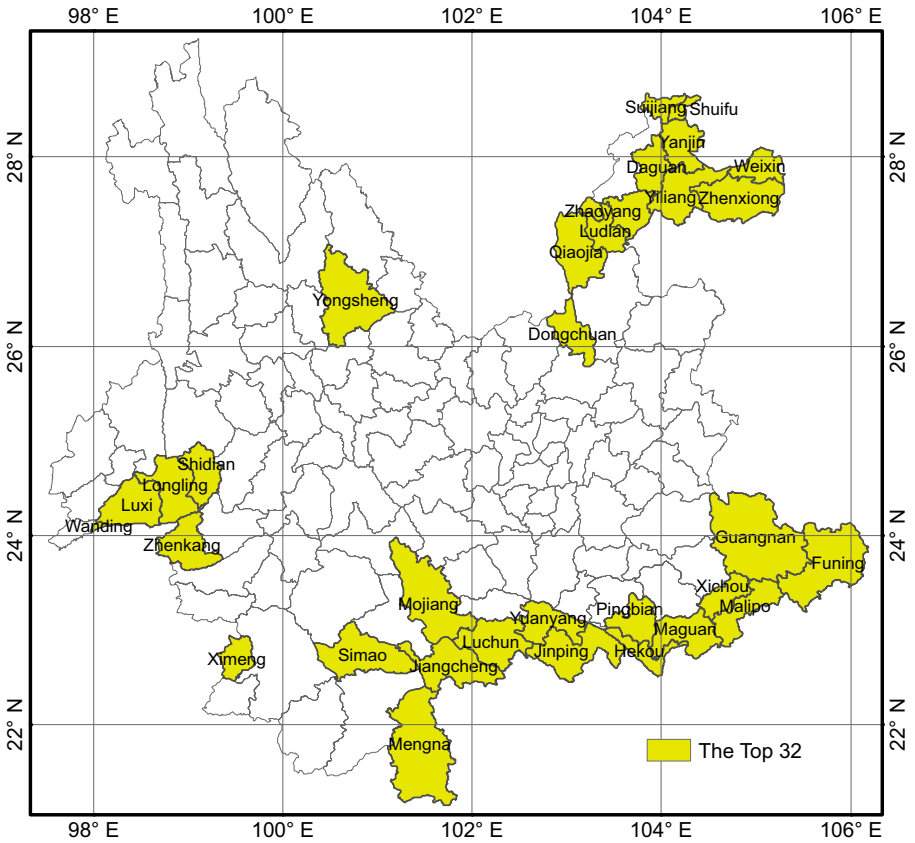

Fig. 9 Top 32 counties with the highest risk of Yunnan Province

categories (e.g., Sarkar and Kanungo 2004). Figure 8b, c shows the histogram of FFRI and four categories. The categories of high and very high risk account for 26.10 and 8.71 % out of the total areas, respectively (Table 5). More than half of the areas in Yunnan are placed into low- and moderate-flash-flood-prone categories.

We listed the top 32 counties with the highest flash flood risk, of which the value of k_j is among the highest (Table 6). Large parts of these counties indicate high flash flood risk, and their locations are shown in Fig. 9. Comparing the mean numeric value of each county's grids for each data type, the three dominant data types were determined for each county. All of the top 10 counties are located in the east Yunnan, with rainfall (Max 6 h and Max 24 h) and flood prevention measures being the common dominant data types. For some counties (e.g., Ximeng, Shidian) in the west Yunnan, vegetation cover and soil contribute most to the risk of flash floods. Additionally, among all the top 32 counties, values for GDP and population are relatively low, which agrees with the fact that flash flooding usually occurs in mountainous areas rather than cities. Meanwhile, in most of the counties, flood prevention measures were poorly implemented.

4 Conclusion and discussion

The major outcome of this work is the development of the CFFG system, which demonstrates the possibilities of flash flood occurrence in a fine resolution at a cascading manner (i.e., from potential to hazard and risk). This study used an integrated weighting method based on the AHP and information entropy theory to derive weights for different data types in the calculation of FFPI, FFHI, and FFRI. The final FFRI values are the weighted linear summation of the vegetation cover, slope, soil, land cover, rainfall amount, GDP, population and flood prevention measures. The CFFG system offers a guideline to determine and assess the distribution of flash flood possibilities based on the available data types in a progressive manner, and it will provide a useful new tool for research and evaluation of flash flood occurrence in areas prone to flash floods.

From the FFPI, FFHI to FFRI, the values of Rank (the skill indicator) are 82.1, 70.8, and 71.8 %, respectively, which imply an overall robustness of the CFFG system in mapping flash flood occurrences. Results show that the CFFG system can further highlight the flash flood hot spots from the high-risk counties successfully, especially in the northeast and southeast of Yunnan. The CFFG methodology is straightforward and useful in explaining the relationship between each data type and flash flood occurrence, with rainfall, flood prevention measures, and geo-topographical conditions showing higher importance for flash flood occurrence in Yunnan.

Compared with other traditional flash flood guidance methods, the CFFG system has more flexibility for expanded applications in China. Future work can be focused on the following: (1) The CFFG system can be updated and applied to other regions when new or finer data sets become available. For instance, the occurrence of wildfire can alter soil water retention capacities and consequently reduce the vegetation cover percentage in some regions (Parsons 2003); (2) more observed flash flood events must be collected to expand this CFFG system to other provinces or even the whole China, as they would allow for the validation of more detailed information.

Acknowledgments This study is partially supported by technical service projects of the China Meteorological Administration, "Technical Research on Meteorological Risk Warning of Flash Floods" (Grant

Number: 20142661168) and "Development and Transformation of a Multi-scale Meteorological Disaster Chain Forecasting Model in China" (Grant Number: 20151451484).

References

Adger V (2006) Vulnerability. Glob Environ Change 16:268–281

Boyle DP (2001) Multicriteria calibration of hydrologic models. Dissertation, Department of Hydrology and Water Resources, University of Arizona

Brans JP, Vincke P, Mareschal B (1986) How to select and how to rank projects: the PROMETHEE method. Eur J Oper Res 24(2):228–238. doi:10.1016/0377-2217(86)90044-5

Brooks N (2003) Vulnerability, risk and adaptation: a conceptual framework. Tyndall Centre for Climate Change Research Working Paper 38:1–16

Büchele B, Kreibich H, Kron A, Thieken A, Ihringer J, Oberle P, Nestmann F (2006) Flood-risk mapping: contributions towards an enhanced assessment of extreme events and associated risks. Nat Hazards Earth Syst Sci 6(4):485–503. doi:10.5194/nhess-6-485-2006

Bumash RJC, Ferral RL, McGuire RA (1973) A generalized streamflow simulation system-conceptual modeling for digital computers. US Department of Commerce, National Weather Service and State of California, Department of Water Resources

Chen H, Yang D, Hong Y, Gourley JJ, Zhang Y (2013) Hydrological data assimilation with the ensemble square-root-filter: use of streamflow observations to update model states for real-time flash flood forecasting. Adv Water Resour 59:209–220. doi:10.1016/j.advwatres.2013.06.010

Clark RA, Gourley JJ, Flamig ZL, Hong Y, Clark E (2014) CONUS-wide evaluation of national weather service flash flood guidance products. Weather Forecast 29(2):377–392. doi:10.1175/WAF-D-12-00124.1

Creutin JD, Borga M, Gruntfest E, Lutoff C, Zoccatelli D, Ruin I (2013) A space and time framework for analyzing human anticipation of flash floods. J Hydrol 482:14–24. doi:10.1016/j.jhydrol.2012.11.009

De Roo A, Barredo JI, Lavalle C, Bodis K, Bonk R (2007) Potential flood hazard and risk mapping at pan-European scale. In: Digital terrain modelling development and applications in a policy support environment, pp 183–202

DHA U (1992) Internationally agreed glossary of basic terms related to disaster management. UN DHA (United Nations Department of Humanitarian Affairs), Geneva

Fuchs S (2009) Susceptibility versus resilience to mountain hazards in Austria-paradigms of vulnerability revisited. Nat Hazards Earth Syst Sci 9:337–352

Georgakakos KP (1987) Real-time flash flood prediction. J Geophys Res Atmos 92(D8):9615–9629

Hapuarachchi HAP, Wang QJ, Pagano TC (2011) A review of advances in flash flood forecasting. Hydrol Process 25(18):2771–2784. doi:10.1002/hyp.8040

Hong Y, Adler R, Huffman G (2007) Use of satellite remote sensing data in the mapping of global landslide susceptibility. Nat Hazards 43(2):245–256. doi:10.1007/s11069-006-9104-z

Hong Y, Adhikari P, Gourley JJ (2013) Flash flood. Encyclopedia of natural hazards. Springer, The Netherlands, pp 324–325

Jiang JH, Shao LP (2010) Standard of mountain flood warning based on the precipitation observation data. J Hydraul Eng 41(4):458–463 **(in Chinese)**

Jiang W, Deng L, Chen L, Wu J, Li J (2009) Risk assessment and validation of flood disaster based on fuzzy mathematics. Prog Nat Sci 19(10):1419–1425. doi:10.1016/j.pnsc.2008.12.010

Karmeshu (2003) Entropy measures, maximum entropy principle and emerging applications. Springer Science & Business Media, vol 119

Khan SI, Adhikari P, Hong Y, Vergara H et al (2011) Hydroclimatology of Lake Victoria region using hydrologic model and satellite remote sensing data. Hydrol Earth Syst Sci 15(1):107–117. doi:10.5194/hess-15-107-2011

Koren V, Reed S, Smith M, Zhang Z, Seo DJ (2004) Hydrology laboratory research modeling system (HL-RMS) of the US national weather service. J Hydrol 291(3):297–318. doi:10.1016/j.jhydrol.2003.12.039

Lee G, Jun KS, Chung ES (2013) Integrated multi-criteria flood vulnerability approach using fuzzy TOPSIS and Delphi technique. Nat Hazards Earth Syst Sci 13(5):1293–1312. doi:10.5194/nhess-13-1293-2013

Li K, Wu S, Dai E, Xu Z (2012) Flood loss analysis and quantitative risk assessment in China. Nat Hazards 63(2):737–760. doi:10.1007/s11069-012-0180-y

Lin X, Lin Q, Wang M, Zhao Y, Li Y (2015) Hazard zoning of flash flood in mountainous administrative region of town: a case study on Tiaoshi Town. J Nat Disasters 3(24):90–96 **(in Chinese)**

Linstone HA, Turoff M (eds) (1975) The Delphi method: Techniques and applications, vol 29. Addison-Wesley, Reading

Long D, Shen YJ, Sun AY, Hong Y, Longuevergne L, Yang YT, Li B, Chen L (2014) Drought and flood monitoring over a large karst plateau in Southwest China using extended GRACE data. Remote Sens Environ 155:145–160

Mogil HM, Monro JC, Groper HS (1978) NWS's flash flood warning and disaster preparedness programs. Bull Am Meteorol Soc 59(6):690–699. doi:10.1175/1520-0477(1978)059<0690:NFFWAD>2.0.CO;2

Papaioannou G, Vasiliades L, Loukas A (2015) Multi-criteria analysis framework for potential flood prone areas mapping. Water Resour Manage 29(2):399–418. doi:10.1007/s11269-014-0817-6

Parsons A (2003) Burned area emergency rehabilitation (BAER) soil burn severity definitions and mapping guidelines Draft. USDA forest service, Rocky Mountain Research Station, Missoula

Pradhan B (2010) Flood susceptible mapping and risk area delineation using logistic regression, GIS and remote sensing. J Spatial Hydrol 9(2):1–18

River Forecast Center Development Management Team (2003) Flash flood guidance improvement team-final report. Report to the operations subcommittee of the NWS corporate board. http://www.nws.noaa.gov/oh/rfcdev/docs/ffgitreport.pdf

Saaty RW (1987) The analytic hierarchy process-what it is and how it is used. Math Modell 9(3):161–176

Saaty TL (1990) How to make a decision: the analytic hierarchy process. Eur J Oper Res 48(1):9–26

Sahoo GB, Ray C (2006) Flow forecasting for a Hawaii stream using rating curves and neural networks. J Hydrol 317(1):63–80. doi:10.1016/j.jhydrol.2005.05.008

Sarkar S, Kanungo DP (2004) An integrated approach for landslide susceptibility mapping using remote sensing and GIS. Photogramm Eng Remote Sens 70(5):617–625

Scheuer S, Haase D, Meyer V (2011) Exploring multicriteria flood vulnerability by integrating economic, social and ecological dimensions of flood risk and coping capacity: from a starting point view towards an end point view of vulnerability. Nat Hazards 58(2):731–751. doi:10.1007/s11069-010-9666-7

Schmidt JA, Anderson AJ, Paul JH (2007) Spatially-variable, physically-derived flash flood guidance. AMS 21st conference on hydrology, San Antonio, TX B, vol 6

Sinha R, Bapalu GV, Singh LK, Rath B (2008) Flood risk analysis in the Kosi river basin, north Bihar using multi-parametric approach of analytical hierarchy process (AHP). J Indian Soc Remote Sens 36(4):335–349. doi:10.1007/s12524-008-0034-y

Smith G (2003) Flash flood potential: determining the hydrologic response of FFMP basins to heavy rain by analyzing their physiographic characteristics. Available from the NWS Colorado Basin River Forecast Center. http://www.cbrfc.noaa.gov/papers/ffp_wpap.pdf

Smith GE (2010) Development of a flash flood potential index using physiographic data sets within a geographic information system. Doctoral dissertation, University of Utah

Store R, Kangas J (2001) Integrating spatial multi-criteria evaluation and expert knowledge for GIS-based habitat suitability modelling. Landsc Urban Plann 55(2):79–93. doi:10.1016/S0169-2046(01)00120-7

Sun D, Zhang D, Cheng X (2012) Framework of national non-structural measures for flash Flood disaster prevention in China. Water 4(1):272–282. doi:10.3390/w4010272

Sweeney TL (1992) Modernized areal flash flood guidance. US Department of Commerce, National Oceanic and Atmospheric Administration, National Weather Service, Office of Hydrology

Sweeney TL, Baumgardner TF (1999) Modernized flash flood guidance. NWS Office of Hydrology, Web Site Version, Updated 8, pp 16–99

Tan H, Ping W, Yang T, Li S, Liu A, Zhou J, Sun Z (2007) The synthetic evaluation model for analysis of flooding hazards. Eur J Public Health 17(2):206–210. doi:10.1093/eurpub/ckl067

Tang C, Zhu J (2005) A GIS based regional torrent risk zonation. Acta Geograph Sinica 60(1):87–94 **(in Chinese)**

Vaidya OS, Kumar S (2006) Analytic hierarchy process: an overview of applications. Eur J Oper Res 169(1):1–29. doi:10.1016/j.ejor.2004.04.028

Villagran de Leon JC (2006) Vulnerability—a conceptual and methodological review. UNU EHS, no 4/2006, Bonn, Germany

Wang J, Hong Y, Li L, Gourley JJ, Khan SI, Yilmaz KK et al (2011a) The coupled routing and excess storage (CREST) distributed hydrological model. Hydrol Sci J 56(1):84–98. doi:10.1080/02626667.2010.543087

Wang Y, Li Z, Tang Z, Zeng G (2011b) A GIS-based spatial multi-criteria approach for flood risk assessment in the Dongting Lake Region, Hunan, Central China. Water Resour Manage 25(13):3465–3484. doi:10.1007/s11269-011-9866-2

Zahedi F (1986) The analytic hierarchy process-a survey of the method and its applications. Interfaces 16(4):96–108

Zhang X, Luo J, Chen L et al (2000) Zoning of Chinese flood hazard risk. J Hydraul Eng 3:3–9 **(in Chinese)**

Zhou G, Yan H (2007) The spatial and temporal distribution feature of precipitation field over Yunnan. J Yunnan Univ Nat Sci 29(1):55 **(in Chinese)**

Zou ZH, Yi Y, Sun JN (2006) Entropy method for determination of weight of evaluating indicators in fuzzy synthetic evaluation for water quality assessment. J Environ Sci 18(5):1020–1023. doi:10.1016/S1001-0742(06)60032-6